Near-field tsunami forecasting using offshore tsunami data from the 2011 off the Pacific coast of Tohoku Earthquake

Hiroaki Tsushima[1], Kenji Hirata[1], Yutaka Hayashi[1], Yuichiro Tanioka[2], Kazuhiro Kimura[1], Shin'ichi Sakai[3], Masanao Shinohara[3], Toshihiko Kanazawa[3], Ryota Hino[4], and Kenji Maeda[1]

[1]*Meteorological Research Institute, Japan Meteorological Agency, 1-1 Nagamine, Tsukuba, Ibaraki 305-0052, Japan*
[2]*Institute of Seismology and Volcanology, Hokkaido University, Kita 10 Nishi 8, Kita-ku, Sappopro 060-0810, Japan*
[3]*Earthquake Research Institute, University of Tokyo, 1-1-1, Yayoi, Bunkyo-ku, Tokyo 113-0032, Japan*
[4]*Research Center for Prediction of Earthquakes and Volcanic Eruptions, Graduate School of Science, Tohoku University, 6-6 Aramaki-Aza Aoba, Sendai 980-8578, Japan*

(Received April 7, 2011; Revised June 29, 2011; Accepted June 30, 2011; Online published September 27, 2011)

Tsunami heights greater than 4 m were observed at several coastal tide-gauge stations during the tsunami generated by the 2011 off the Pacific coast of Tohoku Earthquake (M_w 9.0), causing thousands of casualties and damaging infrastructure along the Pacific coast of Japan. We retrospectively applied an algorithm of near-field tsunami forecasting to tsunami data that were recorded at various offshore tsunami stations 5–10 min before the tsunami reached the coastal tide-gauge stations nearest to its source. We inverted the waveform data recorded offshore to estimate the distribution of the initial sea-surface height, and then tsunami waveforms were synthesized from the estimated source to forecast tsunami arrival times and amplitudes at coastal tide-gauge stations. As a result of a retrospective application made 20 min after the earthquake, tsunamis with heights of 6–14 m were forecasted at tide-gauge stations nearest to the source where the sea-level increase due to the actual tsunami began to exceed 1 m after an elapsed time of 25 min. The result suggests a possibility that the forecasting method we used could contribute to the issuing of reliable near-field tsunami warning for M_w 9 earthquakes.
Key words: Near-field tsunami forecasting, ocean-bottom pressure gauge, GPS buoy, tsunami waveform inversion.

1. Introduction

On 11 March, 2011, the 2011 off the Pacific coast of Tohoku Earthquake (the 2011 Tohoku earthquake, hereafter) occurred along the Japan Trench subduction zone. The source parameters of the earthquake provided by the Japan Meteorological Agency (JMA) were: origin time, 05:46 (UTC); epicenter, 38.0°N, 142.9°E; JMA magnitude (M_{JMA}) 7.9, which was based on the analysis of short-period (several seconds) seismic waves. After detailed analysis of the long-period (longer than several tens of seconds) seismic waves, JMA reported a moment magnitude (M_w) of 9.0 for the earthquake. The large tsunami generated by the earthquake caused severe damage and loss of life over wide areas along the Pacific coast of Japan. Tsunami heights exceeded 4 m at coastal tide-gauge stations near the tsunami source. For example, a water rise of more than 9 m was observed at the tide-gauge station Soma, which is located on the southern part of Tohoku.

In Japan, JMA functions to issue tsunami warnings within a few minutes of an earthquake based on the rapid analysis of seismic wave data (Tatehata, 1997). The initial warnings are sometimes updated taking into consideration observed tsunami heights at offshore tsunami stations or coastal tide-gauge stations. At 3 min after the 2011 Tohoku earthquake, tsunami warnings or advisories were issued for wide areas of the Pacific coast along the Japan Trench. For example, JMA initially forecast that tsunamis of 3–6 m height (or larger in some locations) would affect coastal regions near to the earthquake source. Twenty-eight minutes after the earthquake, forecasted tsunami heights for these coastal regions were updated to 6–10 m or more. At 45 min, JMA again updated the warnings to the effect that tsunami heights of more than 10 m were more widely expected in coastal areas along the Japan Trench.

These large tsunamis were clearly observed at offshore tsunami observation stations around Japan, such as cabled ocean-bottom pressure gauges (OBPGs) (e.g., Meteorological Research Institute, 1980) and GPS buoys (e.g., Kato *et al.*, 2005), as well as by the worldwide Deep-ocean Assessment and Reporting of Tsunamis (DART) buoy systems (e.g., Titov *et al.*, 2005). Because tsunamis can be detected at offshore stations earlier than at the coast, several methods of tsunami forecasting based on offshore tsunami data have been proposed for near-field tsunamis (e.g., Baba *et al.*, 2004; Takayama, 2008; Tatsumi and Tomita, 2009; Tsushima, 2009; Tsushima *et al.*, 2009; Hayashi, 2010), as well as for far-field tsunamis (Titov *et al.*, 2005). In the present paper, we focus on forecasting near-field tsunamis. Near-field tsunamis in areas close to subduction zones can reach the coast in a few tens of minutes, or less, and can cause catastrophic damage. Therefore,

doi:10.5047/eps.2011.06.052

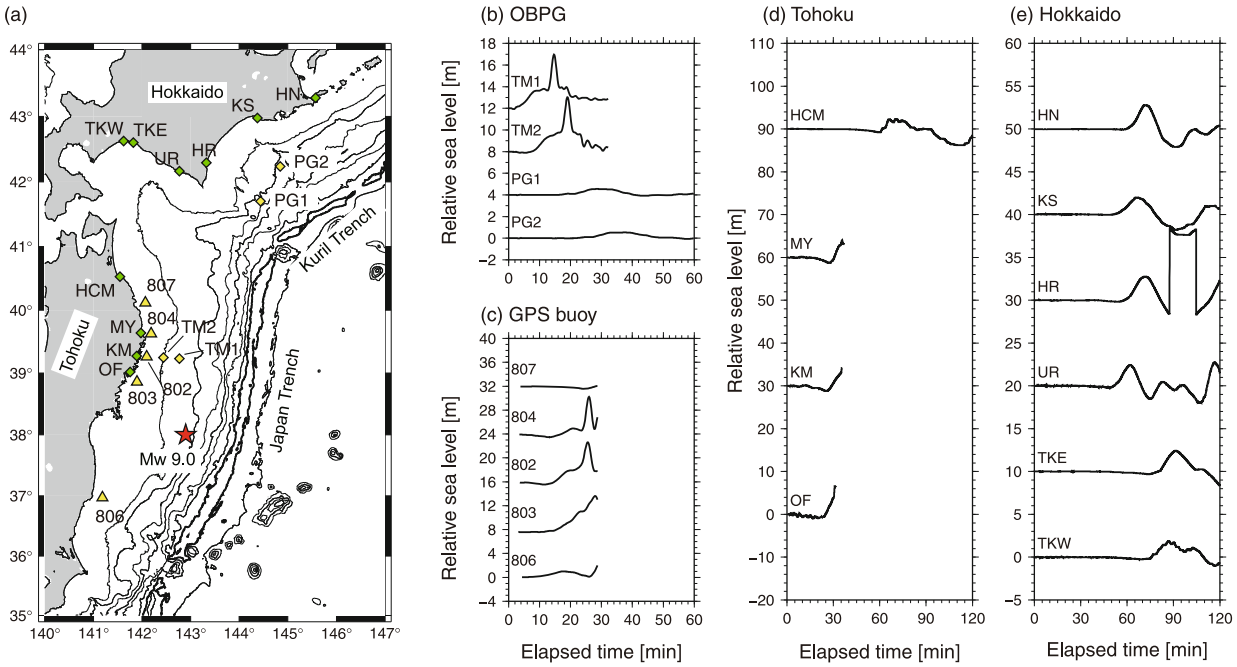

Fig. 1. (a) Map of the study area showing the locations of cabled OBPGs, GPS buoys, and coastal tide-gauge stations used in this study. The red star indicates the epicenter of the 2011 Tohoku earthquake as estimated by JMA. The OBPG, GPS buoy and tide-gauge stations are indicated by yellow diamonds, yellow triangles, and green diamonds, respectively. Waveforms recorded after the 2011 Tohoku earthquake at (b) four OBPG stations, (c) five GPS buoy stations, (d) four coastal tide-gauge stations in northern Tohoku, and (e) six coastal tide-gauge stations in Hokkaido.

the time window for issuing warnings of arrival times and amplitudes of near-field tsunamis is much shorter than that for far-field tsunamis. Despite this difficulty, the development of a system to provide reliable forecasts of tsunamis caused by local earthquakes is important for the effective mitigation of damage and loss of life in coastal communities.

We have retrospectively examined how rapidly and accurately tsunami forecasts were provided from real-time data assimilation (inversion) of the offshore tsunami waveform data following the 2011 Tohoku earthquake. We have then considered possible improvements to the present tsunami-forecasting algorithm.

2. Data

After the 2011 Tohoku earthquake, tsunami waveforms were recorded off the Pacific coast in the Tohoku and Hokkaido regions at four OBPGs, TM1 and TM2 (Kanazawa and Hasegawa, 1997) and PG1 and PG2 (Hirata *et al.*, 2002). They were also recorded at five GPS buoys (802, 803, 804, 806, and 807) (Figs. 1(a), 1(b), and 1(c)). These tsunami data are usually transmitted to the data center of JMA in real time for the purpose of tsunami monitoring. When the 2011 Tohoku earthquake occurred, however, the later part of those waveform data at most stations (TM1, TM2, and all the GPS buoys) were not available on a real-time basis because of problems caused by strong ground motion and large tsunami, such as the disruptions of landing stations for the cabled system (Figs. 1(b) and 1(c)). In addition, at that time it was reported that the positioning accuracies of the initial parts of the GPS buoy data were low because of the strong ground motion (Fig. 1(c)). For this study, we have retrospectively applied an algorithm of tsunami forecasting to the data that were available in real time (Figs. 1(b) and 1(c)).

The pressure data recorded by the OBPGs include the effect of ocean tides, atmospheric and oceanographic disturbances, and seismic waves, as well as tsunamis and the vertical deformation of the seafloor, that are used for the inversion. For example, when the 2011 Tohoku earthquake occurred, at the OBPG station TM1 a very large pressure fluctuation ($\sim$80 m in equivalent water depth) with a period of $\sim$10 s which was probably due to seismic waves and/or water column oscillation (e.g., Nosov and Kolesov, 2007) was recorded, in addition to the tsunami and/or seafloor deformation. The pressure variations due to tsunami and coseismic seafloor deformation have very different time scales from those of the other phenomena, and therefore we can separate them easily. To extract the required components from the original OBPG data, we followed Tsushima *et al.* (2009) to apply a 60-s moving average, low-pass digital filter with a cut-off period of 60 s (Saito, 1978), and a tide correction based on a theoretical tide model of Matsumoto *et al.* (2000). After the data-processing procedure is carried out, the required components are obtained as shown in Fig. 1(b).

In records from stations TM1 and TM2, the sea-level variation (or water-depth change) due to the permanent seafloor deformation (subsidence) and/or due to the tsunami began to be evident soon after the earthquake occurred (Fig. 1(b)). At TM1, the gradual sea-level increase was recorded from the origin time to $\sim$12 min, followed by impulsive tsunami. The gradual variation probably includes both the contribution of the sea-surface movement to return to the sea level increasing by the amount of the seafloor subsidence, and that of the tsunami propagating from the

surrounding uplifted area. At TM2, the gradual sea-level decrease was recorded from the origin time to ∼10 min, and then the similar sea-level variation to that at TM1 was measured. The first decreasing variation would be due to a tsunami propagating from the surrounding subsidence area. Following the impulsive tsunami arrival, the sea-level increase reaches ∼5 m at ∼15 min (TM1) and 20 min (TM2), while at the coastal tide-gauge station Ofunato (OF), near the earthquake epicenter, the sea-level increase due to the tsunami started to exceed 1 m ∼25 min after the earthquake (Fig. 1(d)). The tsunami reached offshore stations PG1 and PG2 off Kushiro, Hokkaido, about 20–25 min after the earthquake (Fig. 1(b)).

The data from GPS buoys are recorded by the Port and Airport Research Institute (PARI), and the first tens of minutes of real-time waveform data were available almost immediately after the earthquake. When the 2011 Tohoku earthquake occurred, the GPS buoys deployed in the Tohoku region measured the vertical sea-surface movement due to the coseismic seafloor deformation below the GPS buoy (i.e. the initial sea-surface displacement), and that due to the propagating tsunami. The sea level started to change within 10 min after the earthquake at all the GPS buoys (Fig. 1(c)): a few minutes after the earthquake at GPS buoys 802, 803, and 804, ∼5 min at buoy 806, and ∼10 min at buoy 807. Moreover, at three GPS buoys 802, 803, and 806, sea-surface displacements more than 1 m were observed ∼7 min earlier than at the coastal tide gauge station OF.

To evaluate the performance of our tsunami forecasting method, we compared the waveforms forecasted by our inversion with tsunami waveforms observed at 10 coastal tide-gauge stations, four in northern Tohoku (Hachinohe, HCM; Miyako, MY; Kamaishi, KM; and Ofunato, OF) (Fig. 1(d)), and six in Hokkaido (Hanasaki, HN; Kushiro, KS; Hiroo, HR; Urakawa, UR; Tomakomai East, TKE; and Tomakomai West, TKW) (Fig. 1(e)). At tide-gauge stations MY, KM, and OF in Tohoku, sea-level data recording ceased shortly after the arrival of large 4–7-m tsunamis that destroyed their recording systems. At tide-gauge stations in Hokkaido, the observed tsunamis were greater than 1 m in height.

3. Method

To retrospectively forecast the coastal tsunamis generated by the 2011 Tohoku earthquake, we apply a method of near-field tsunami forecasting developed by Tsushima *et al.* (2009), named "tsunami Forecasting based on Inversion for initial sea-Surface Height" (tFISH). For the tFISH algorithm, offshore tsunami-waveform data are inverted to determine the distribution of initial sea-surface height in a possible tsunami source region, and then coastal tsunami waveforms are synthesized from the estimated initial sea-surface height and pre-computed tsunami Green's functions.

A feature of tFISH is that the initial sea-surface height distribution is estimated, not the slip distribution along an assumed fault plane. This approach allows us to estimate a tsunami source without knowing the geometry of the fault that initiated the tsunamigenic earthquake. This is an advantage when we forecast tsunamis generated by normal faults in the trench outer slope region and splay faults. As well as fault geometry, no assumptions concerning the size of an earthquake (e.g., a seismic moment) are required in tFISH. The use of such parameters may bias the estimation of tsunami sources, which is undesirable for tsunami forecasts in the cases of tsunami earthquakes.

In tFISH, the predictions are repeated by progressively updating the offshore tsunami-waveform data. Because individual predictions can be calculated in less than one minute, tsunami predictions can be updated at short intervals of time, thus providing successive tsunami predictions with improved accuracy.

For the tFISH algorithm, the area over which the initial sea-surface displacement is estimated (the "influence area", hereafter) is defined as the area surrounded by the back-propagated wavefronts from each of the offshore tsunami stations that is based on the full propagation (Tsushima *et al.*, 2009). In the definition of the influence area, we assumed that the origin time of the earthquake, estimated by JMA from seismic data, was the origin time of the tsunami. For the inversion, the smoothing and damping constraints are imposed, as well as in Tsushima *et al.* (2009). The damping constraint is based on *a priori* information about the location of the tsunami source: the initial sea-surface displacement due to an earthquake should be zero if the epicenter is far enough away. The epicenter determined by JMA was applied for the damping constraint. The infinite rupture velocity was assumed, meaning that both the coseismic seafloor deformation and the initial sea-surface displacement started and stopped simultaneously over the whole source region.

To compute the Green's functions, we calculated the finite-difference approximation of the linear long-wave equations in a spherical coordinate system (Satake, 1995). The computation area was set as follows: 30°N–45°N; 140°E–150°E. The grid size was 20 arc seconds (about 600 m) and bathymetry grid data was produced from the following bathymetry data: J-EGG500 provided by the Japan Oceanographic Data Center (500-m grid interval), JTOPO30 by the Marine Information Research Center, the Japan Hydrographic Association (30-arc-seconds grid interval). The grid size near coastal tide-gauge stations was set to 4 arc seconds as nested grids. The time step for the computation was 1 s to satisfy the stability condition. A single element of the initial sea-surface height for the computation of the Green's functions (an elemental tsunami source, hereafter) was represented by a square of dimensions 700 × 700 arc seconds with stair-like steps. The rise time was set to 10 s. These settings were the same as those of Tsushima *et al.* (2009).

The effect of a permanent vertical deformation of the seafloor on the OBPG records was taken into account in the Green's functions by applying the method of Tsushima (2009) to the Green's functions. The correction factor to be provided for the original Green's functions can be obtained easily from an elemental tsunami source. Thus, the correction technique can be applied immediately after the original Green's functions are computed, and the revised Green's functions are applicable in our real-time approach.

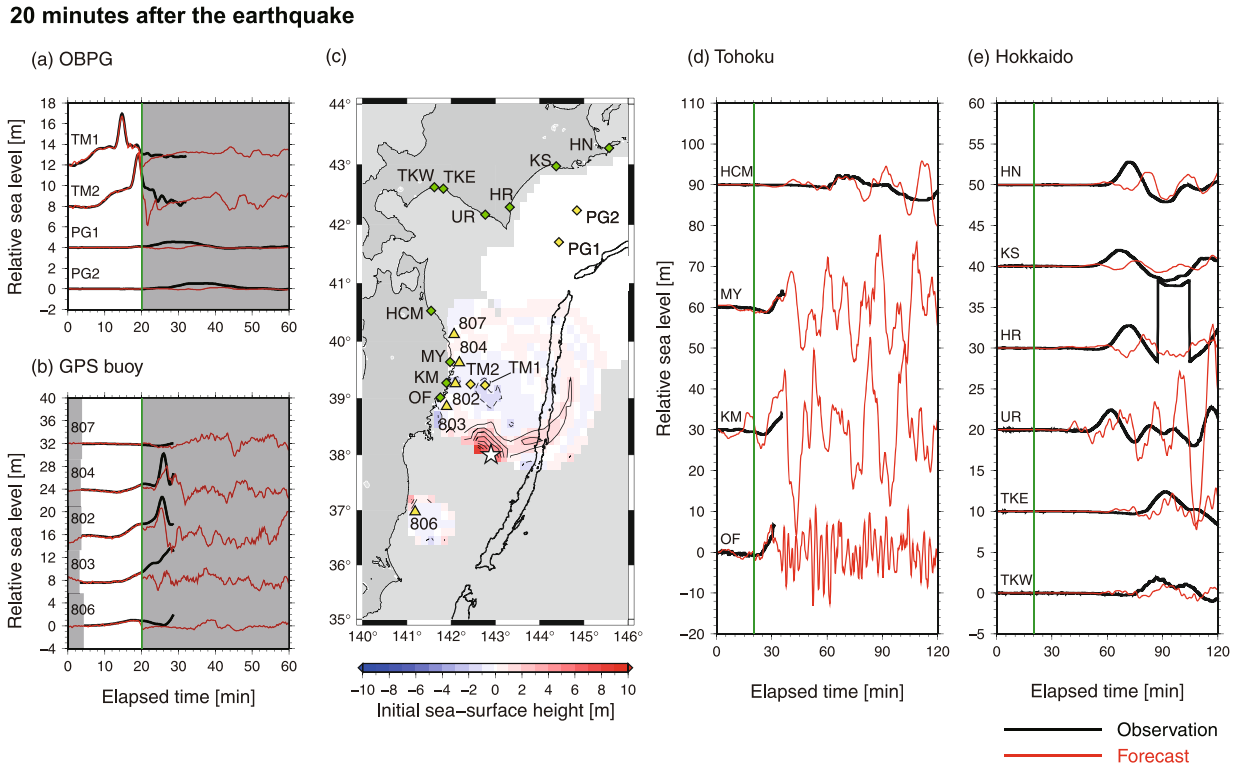

Fig. 2. Result of a retrospective tFISH tsunami forecast 20 min after the 2011 Tohoku earthquake. Comparison of observed (black lines) and calculated (red lines) waveforms at (a) four OBPGs and (b) five GPS buoys. The waveforms in the unshaded areas of each panel were used in the inversion. (c) Distribution of the initial sea-surface height estimated by tsunami-waveform inversion. The star indicates the earthquake epicenter used as the damping constraint in the inversion. The areas shaded gray are outside the influence area. The contour interval is 1 m. Comparison of observed (black lines) and forecasted (red lines) tsunami waveforms at coastal tide-gauge stations in (d) northern Tohoku and (e) Hokkaido. Vertical green lines in (a), (b), (d) and (e) indicate the time of the forecast.

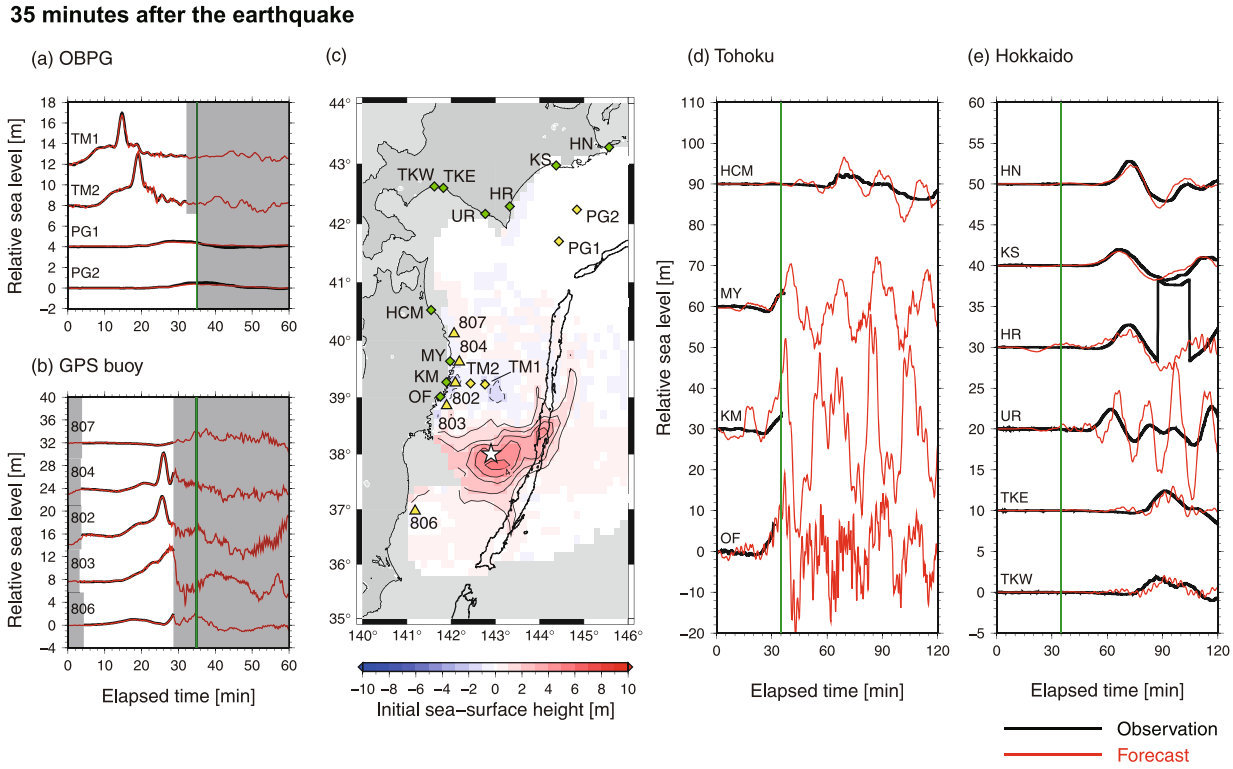

Fig. 3. Result of the retrospective tFISH tsunami forecast 35 min after the 2011 Tohoku earthquake. See Fig. 2 for details of panels (a) to (e).

4. Results

We first examined the accuracy of a retrospective tsunami forecast using the first 20 min of data from the 2011 Tohoku earthquake. A comparison of the forecasted tsunami waveform (red lines) with the observed waveforms (black lines) is shown in Fig. 2. At this time, the first peaks of the tsunamis had been recorded at offshore stations TM1 and TM2 (Fig. 2(a)) and the initial sea-surface elevations due to the tsunami had been measured at GPS buoys 802, 803, 804, and 806 (Fig. 2(b)). These observations help to estimate the large elevation of the sea surface around the epicenter (Fig. 2(c)), providing a constraint for the forecasted amplitudes of the tsunami. For the northern Tohoku coastal region, the first peak amplitudes of the tsunamis were forecasted to be ∼2 m at tide-gauge station HCM, ∼9 m at MY, 10–14 m at KM, and ∼6.5 m at OF (Fig. 2(d)). At stations MY, KM, and OF, the forecasted onsets of the first tsunamis roughly match the observations. These retrospective results indicate that tFISH could have provided information that disastrous tsunami heights larger than 5–10 m were approaching communities along the Pacific coast of northern Tohoku, more than 5 min before the actual tsunami attack. However, we cannot evaluate the accuracy of our tsunami forecasts quantitatively because data recording stopped before the first tsunami peak at most of the tide-gauge stations (Fig. 2(d)). The accuracy of the tsunami forecasts at the tide-gauge stations on the Hokkaido coast was low (Fig. 2(e)).

Next, we examined the accuracy of our retrospective tsunami forecasts at an elapsed time of 35 min. At offshore stations PG1 and PG2, the sea-surface elevations due to the first tsunamis had been recorded (Fig. 3(a)). Also, at GPS buoys 802, 803, and 804, the first peaks of the tsunamis had been recorded (Fig. 3(b)). The estimated sea-surface elevation area extends in a roughly circular pattern from the epicenter to the Japan Trench (maximum elevation 5.7 m) (Fig. 3(c)), also shown in Fig. 2(c). A more detailed discussion about the estimated source will be presented in the next section. At tide-gauge stations MY, KM, and OF on the northern Tohoku coast, the forecasted heights of the first tsunamis were greater than 10 m, while the actual heights already reached larger than 4 m at this time (Fig. 3(d)). In comparison, the tsunami-waveform forecasts at all the tide-gauge stations in the Hokkaido region match the observations well (Fig. 3(e)), perhaps helped by the contributions of the observations at stations PG1 and PG2 to the inversion. These results show that the tFISH algorithm could have provided more accurate tsunami forecasts for the coastal communities of Hokkaido than at an elapsed time of 20 min with lead times of more than 10 min.

5. Discussions and Conclusions

Our retrospective experiments suggest that tFISH could have provided tsunami information, with a lead time of more than 5 min, of 5–10-m tsunami heights from the 2011 Tohoku earthquake along the Pacific coast in northern Tohoku, although the accuracy of the forecasted first-peak tsunami height cannot be evaluated quantitatively. On the basis of our simulation made 35 min after the earthquake, tFISH would have provided reasonably-accurate forecasts of the heights and arrival times of the first tsunami for the coastal communities in Hokkaido with a lead time of 10 min.

The spatial pattern of the estimated initial sea-surface height distribution tends to be distributed along a set of the back-propagated wavefronts from offshore stations TM1 and TM2, as well as from GPS buoys 802, 803, and 804 (Figs. 2(c) and 3(c)). The spatial pattern indicates that the azimuthal coverage of the offshore stations is not sufficient to constrain the extent of the source area well. The resulting artifact source would degrade the accuracy of the tsunami forecasting. The installation of additional offshore tsunami stations having an appropriate spacing (e.g., Tsushima *et al.*, 2009) can produce a better azimuthal coverage and resolve the problem. If the waveform data recorded at the offshore stations with enough azimuthal coverage are sufficient to estimate an accurate tsunami source model, we would not have to apply the damping constraint in the inversion. The damping constraint tends to lower the inverted displacement at the sea-surface segment where the epicenter is far enough away, while the source areas of M_w 9 earthquakes are huge and the sea surface, where the epicenter is far away, may be substantially displaced by a coseismic fault slip. Therefore, tsunami forecasting without the damping constraint is preferred for M_w 9 earthquakes.

A short-period, large impulsive tsunami was observed around an elapsed time of 14 min for TM1, 16 min for TM2, 24 min for GPS buoy 802, and 25 min for GPS buoy 804 (Figs. 1(b) and 1(c)). To model such short-period tsunamis accurately, a tsunami computation based on the dispersive wave theory (Tanioka, 2000; Saito and Furumura, 2009) will be required, instead of a linear long-wave theory, in the computation of the Green's functions. Use of the dispersive theory will improve the spatial extent of an estimated tsunami source (Saito *et al.*, 2010), resulting in an improvement in the accuracy of coastal tsunami forecasts.

In addition to the dispersion, large tsunamis generated by M_w 9 earthquakes are subject to nonlinear effects. For the forecasting of massive tsunamis, the application of an inversion method based on nonlinear shallow-water equations (e.g., Piatanesi and Lorito, 2007) will be one possible avenue for future improvement. Another possible solution would be the use of tsunami-inundation computation. For near-field tsunamis, an application of a real-time computation of tsunami inundation which is used for far-field tsunamis (Titov *et al.*, 2005) will not be desirable because the lead time is very short. The strategy proposed by Abe and Imamura (2010) will be preferred for the inundation forecasting of near-field tsunamis. In their study, many inundation scenarios are pre-computed before earthquakes occur. Then, after an earthquake occurs, possible scenarios are narrowed down from the pre-computed inundation scenarios by referring information available in real time, such as seismic-source parameters and tsunami observation. The method can reduce real-time computation time. Moreover, a tsunami-source model estimated by our tFISH algorithm can be used in their system as one indicator to choose appropriate inundation scenarios.

The results of this study demonstrate that tFISH has the potential to provide useful tsunami information in real time

for M_w 9 earthquakes. With the implementation of the improvements suggested here, the reliability of tFISH forecasts would be improved and would make a greater contribution to the mitigation of future tsunami disasters.

Acknowledgments. We thank both the Earthquake Research Institute at the University of Tokyo and the Japan Agency of Marine-Earth Science and Technology for providing tsunami data recorded by cabled ocean-bottom pressure sensors. We also thank the Ministry of Land, Infrastructure, Transport and Tourism, and the Port and Airport Research Institute for providing tsunami data from GPS buoys and coastal tide-gauge stations, and the Japan Meteorological Agency and the Japan Coast Guard for providing tsunami data from coastal tide-gauge stations. We are grateful to Dr. Eric Geist and an anonymous reviewer for their critical and constructive comments and suggestions which have improved the manuscript. We thank Dr. Takuto Maeda of the Earthquake Research Institute for helpful discussions. We are also grateful to Dr. Yasuhiro Yoshida, Shigeki Aoki, and Dr. Fuyuki Hirose of the Meteorological Research Institute for their comments and technical support. Our special thanks go to Dr. Hiroyasu Kawai of the Port and Airport Research Institute and Tatsuo Kuwayama of the Japan Meteorological Agency. The figures in this paper were prepared using Generic Mapping Tools (Wessel and Smith, 1991).

References

Abe, I. and F. Imamura, Study on the evaluation of tsunami inundation in real time with database and its accuracy, *J. Jpn. Soc. Civil Eng., Ser. B2 (Coastal Engineering)*, **66**, 261–265, 2010 (in Japanese with English abstract).

Baba, T., K. Hirata, and Y. Kaneda, Tsunami magnitudes determined from ocean bottom pressure gauge data around Japan, *Geophys. Res. Lett.*, **31**, L08303, doi:10.1029/2003GL019397, 2004.

Hayashi, Y., Empirical relationship of tsunami height between offshore and coastal stations, *Earth Planets Space*, **62**, 269–275, 2010.

Hirata, K., M. Aoyagi, H. Mikada, K. Kawaguchi, Y. Kaiho, R. Iwase, S. Morita, I. Fujisawa, H. Sugioka, K. Mitsuzawa, K. Suyehiro, H. Kinoshita, and N. Fujiwara, Real-time geophysical measurements on the deep seafloor using submarine cable in the southern Kurile subduction zone, *IEEE J. Oceanic Eng.*, **27**, 170–181, doi:10.1109/JOE.2002.1002471, 2002.

Kanazawa, T. and A. Hasegawa, Ocean-bottom observatory for earthquakes and tsunami off Sanriku, north-east Japan using submarine cable, *International Workshop on Scientific Use of Submarine Cables, Comm. for Sci. Use of Submarine Cables*, Okinawa, Japan, 208–209,1997.

Kato, T., Y. Terada, K. Ito, R. Hattori, T. Abe, T. Miyake, S. Koshimura, and T. Nagai, Tsunami due to the 2004 September 5th off the Kii peninsula earthquake, Japan, recorded by a new GPS buoy, *Earth Planets Space*, **57**, 297–301, 2005.

Matsumoto, K., T. Takanezawa, and M. Ooe, Ocean tide models developed by assimilating TOPEX/POSEIDON altimeter data into hydrodynamical model: A global model and a regional model around Japan, *J. Oceanogr.*, **56**, 567–581, doi:10.1023/A:1011157212596, 2000.

Meteorological Research Institute, Permanent ocean bottom seismograph observation system, *Tech. Rep. 4*, 233 pp., Tsukuba, Japan, 1980 (in Japanese with English abstract).

Nosov, M. A. and S. V. Kolesov, Elastic oscillations of water column in the 2003 Tokachi-oki tsunami source: in-situ measurements and 3-D numerical modeling, *Nat. Hazards Earth Syst. Sci.*, **7**, 243–249, 2007.

Piatanesi, A. and S. Lorito, Rupture process of the 2004 Sumatra-Andaman earthquake from tsunami waveform inversion, *Bull. Seismol. Soc. Am.*, **97**, S223–S231, doi:10.1785/0120050627, 2007.

Saito, M., An automatic design algorithm for band selective recursive digital filters, *Butsuri Tankou*, **31**, 112–135, 1978 (in Japanese).

Saito, T. and T. Furumura, Three-dimensional simulation of tsunami generation and propagation: Application to intraplate events, *J. Geophys. Res.*, **114**, B02307, doi:10.1029/2007JB005523, 2009.

Saito, T., K. Satake, and T. Furumura, Tsunami waveform inversion including dispersive waves: the 2004 earthquake off Kii Peninsula, Japan, *J. Geophys. Res.*, **115**, B06303, doi:10.1029/2009JB006884, 2010.

Satake, K., Linear and nonlinear computations of the 1992 Nicaragua earthquake tsunami, *Pure Appl. Geophys.*, **144**, 455–470, doi:10.1007/BF00874378, 1995.

Takayama, H., Statistical relationship between tsunami maximum amplitudes of offshore and coastal stations, *Pap. Meteorol. Geophys.*, **59**, 83–95, 2008.

Tanioka, Y., Numerical simulation of far-field tsunamis using the linear Boussinesq equation—The 1998 Papua New Guinea tsunami—, *Pap. Meteorol. Geophys.*, **51**, 17–25, 2000.

Tatehata, H., The new tsunami warning system of the Japan Meteorological Agency, in *Perspectives on Tsunami Hazard Reduction: Theory and Planning*, edited by G. Hebenstreit, pp. 175–188, Kluwer Academic Publishers, 1997 (also in *Sci. Tsunami Hazards*, **16**, 39–49, 1997).

Tatsumi, D. and T. Tomita, Real-time tsunami inundation prediction based on inversion method, *J. Jpn. Soc. Civil Eng., Ser. B2 (Coastal Engineering)*, **65**, 351–355, 2009 (in Japanese with English abstract).

Titov, V. V., F. I. González, E. N. Bernard, M. C. Eble, H. O. Mojfeld, J. C. Newman, and A. J. Venturato, Real-time tsunami forecasting: Challenges and solutions, *Nat. Hazards*, **35**, 35–41, doi:10.1007/s11069-004-2403-3, 2005.

Tsushima, H., Near-field tsunami forecasting from ocean bottom pressure and onshore GPS data, Doctoral dissertation of Tohoku University, 143 pp., 2009.

Tsushima, H., R. Hino, H. Fujimoto, Y. Tanioka, and F. Imamura, Near-field tsunami forecasting from cabled ocean bottom pressure data, *J. Geophys. Res.*, **114**, B06309, doi:10.1029/2008JB005988, 2009.

Wessel, P. and W. H. F. Smith, Free software helps map and display data, *Eos Trans. AGU*, **72**(41), 441, doi:10.1029/90EO00319, 1991.

H. Tsushima (e-mail: tsushima@mri-jma.go.jp), K. Hirata, Y. Hayashi, Y. Tanioka, K. Kimura, S. Sakai, M. Shinohara, T. Kanazawa, R. Hino, and K. Maeda